Scientia Iranica, Vol. 8, No. 1, pp 38–53

SCIENTIA
IRANICA

Semi-Active Multivariable Adaptive Control of Structures under Earthquake Excitations

A.A. Golafshani* and H.R. Mirdamadi[1]

In this paper, a semi-active multivariable adaptive controller is designed for a framed structure under a seismic disturbance using a filtered-x NLMS optimizer. Actuator and large power supply are not required, since just some valves and a battery-size power supply are sufficient for controlling the amount of hydraulic fluid flow through the by-pass on off-orifice channel in an energy dissipating system, which consists of a piston attached to Λ-shaped wind bracing of the building and a cylinder attached to the upper floor. It is assumed that only a rough finite element model of the structure is available. In addition, in order to search for optimal non-classical viscous damper coefficients, acting as calibration measures for the corresponding orifice size of the by-pass channels of dissipation systems, the adaptive controller parameters are estimated by Normalized Least-Mean-Squares strategy. The simulation results demonstrate that even though the controllability offered by this system does not equal that of an active counterpart, it is almost as effective. Considering low-power requirement for the proposed system appears more attractive and practical in real structures.

INTRODUCTION

Semi-active control strategies have been recently suggested as an alternative for passive and active control methodologies applied to civil engineering structures [1], offering some merit over the other methods. Here, the basic differences of these strategies are discussed briefly. In active control strategy, the system is fully intelligent and energetic. It is capable of not only receiving information regarding both its dynamic behavior (structural response) and its environment (external excitations and disturbances) through sensors, but also is capable of making use of external energy through actuators (electric motors, active tendons, AMD's and so on), in order to optimally regulate the response [2]. In semi-active control strategy, the system is fully informative but not energetic. It may receive all the necessary information, but there are no external energy power sources available [3]. In this system, only a small amount of energy is required (several orders of magnitude less than an active one) for changing the internal dynamic characteristics by an on-off switch or by adjusting the diameter of an orifice in a variable-orifice damper in which hydraulic viscous fluid is flowing. In passive control, the system is neither informative nor energetic; i.e., it neither knows nor can change its conditions [3]. Control strategies based on semi-active devices appear to combine the best features of both passive and active control systems and to offer the greatest likelihood for future acceptance of control technology as a viable means of protecting structural systems against earthquake loading.

VARIABLE-ORIFICE ENERGY DISSIPATING MECHANISM

One means of achieving a variable-damping device for dissipating seismic energy is to use controllable electromechanical variable-orifice valves to alter the resistance to the flow of a conventional hydraulic fluid damper [4]. Construction of such a system is highly expensive and requires super high technology.

In another method, converting a passive-type fluid damper device, similar to a typical Taylor device [5], to a hybrid (passive+semi-active) damping device might be considered, as proposed by the authors, through adding a number of by-pass oil intakes that can be switched on and off, via some control signals.

In the proposed mechanism, a proper kind of hydraulic oil (e.g., silicone) is placed in the closed containers into which the oil can flow. A number of

*. *Corresponding Author, Department of Civil Engineering, Sharif University of Technology, Tehran, I.R. Iran.*

1. *Department of Civil Engineering, Sharif University of Technology, Tehran, I.R. Iran.*

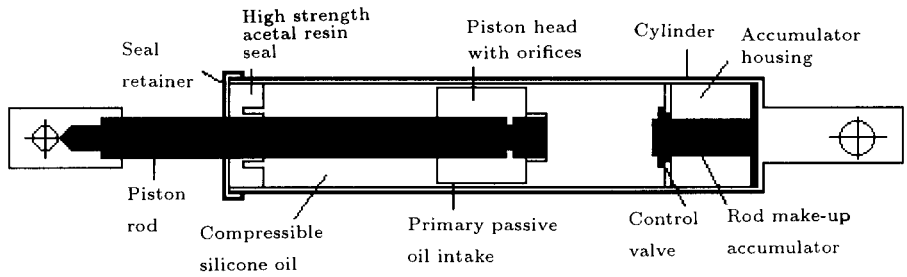

Figure 1. Passive viscous fluid damper of Taylor device.

orifices in the head of each piston provide the direct passive-type channels for the oil flow, similar to the passive-type counterpart. Therefore, there is always some oil flow due to the movement of pistons when drift occurs between adjacent floors. However, there would be some semi-active by-pass oil intakes through which the discharge is regulated by some controlled valves. These valves are powered by battery-size power supplies and are controlled by signals from adaptive filters/controllers. From a mathematical viewpoint, it appears that the damping coefficients of the above-defined energy dissipating system are changing automatically, and an optimal controller is designed to do the regulation adaptively, i.e., based on the latest variations in the frequency domain characteristics of the excitation disturbance. Seismic disturbance is a nonstationary process with a zero mean and a time-variant autocovariance. A schematic of Taylor device, first designed and tested by Constantinou et al. [5], and after that by Symans et al. [6], is provided in Figure 1.

The hybrid version of this device, proposed by the authors, is shown in Figure 2. The function of this hybrid on-off orifice damping device may be interpreted as being similar to a variable-orifice device, using the following mathematical reasoning. By installing three on-off orifice damping devices in a three-floor framed structure (one device at each floor level) and devising

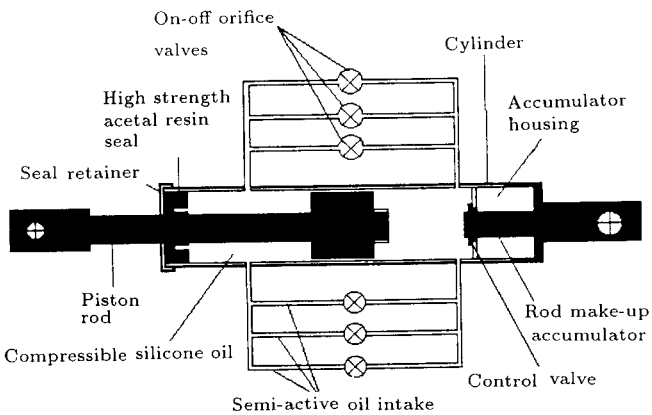

Figure 2. Semi-active on-off orifice viscous fluid damper (proposed by the authors).

six semi-active oil intakes for each device, it is possible to have $2^6 = 64$ distinct values for the nonclassical damping coefficient of each damping device at each time step. By increasing the number of semi-active oil intakes, the number of accessible damping values increases by a geometric progression, very rapidly. Therefore, it may be assumed that the step variation of device damping coefficient is continuous and this on-off orifice device is acting approximately like a variable-orifice system.

THE STRUCTURE MODEL

As a benchmark, a three-story framed-structural building with rigid floors and Λ-shaped wind bracings is considered. The vertices of the bracing systems are attached rigidly to pistons that are free to move horizontally through the cylinders that, in turn, are attached rigidly to the upper floors (see Figure 3).

A rough finite element model of the structural

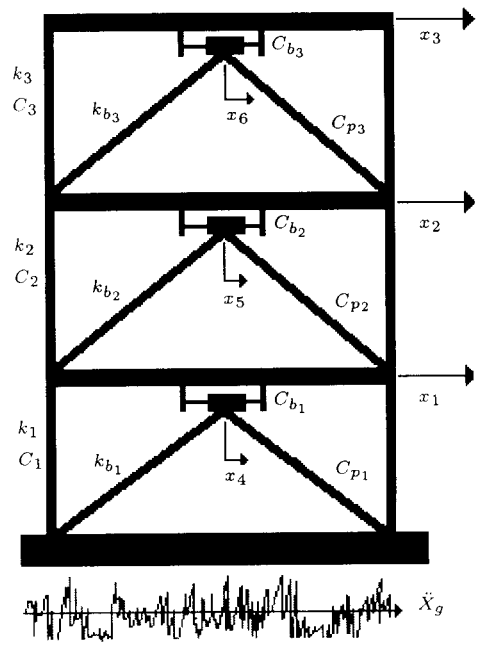

Figure 3. Physical structure.

system is used. The finite element model consists of structural stiffness, consistent mass and damping matrices. The damping matrix consists of two distinct parts: 1) The proportional Rayleigh damping, representing the distributed and nonviscous damping property of the building material; 2) The nonclassical damping, representing a physical local viscous oil flowing through variable-orifice valves. The nonclassical damping is formulated in the state-space time domain description, which is preferred in control design [7].

A multivariable [8,9] three-input three-output, adaptive controller based on normalized filtered-x LMS optimizer [10] is designed. By a heuristic control law, the control forces are converted to some control signals for changing the characteristics of nonclassical damping matrix through controlling the orifice diameters. Inexact structure transfer functions have been used. Due to the adaptive nature of the algorithm, good results have been attained [11,12].

MULTIVARIABLE ADAPTIVE CONTROLLER/LMS OPTIMIZER

The horizontal vibrations of a three-story structure are modeled by only the first six modes of natural vibration. There are three principal DOF's for the floors and another three for the vertices of Λ-bracing (see Figures 3 and 4). The second-order matrix equation of the reduced model is written as follows [13]:

$$\mathbf{M}\ddot{\mathbf{x}} + \mathbf{C}_p\dot{\mathbf{x}} + \mathbf{C}_b(t)\dot{\mathbf{x}} + \mathbf{k}\mathbf{x} = -\mathbf{M}\mathbf{r}_g\ddot{x}_g(t), \qquad (1)$$

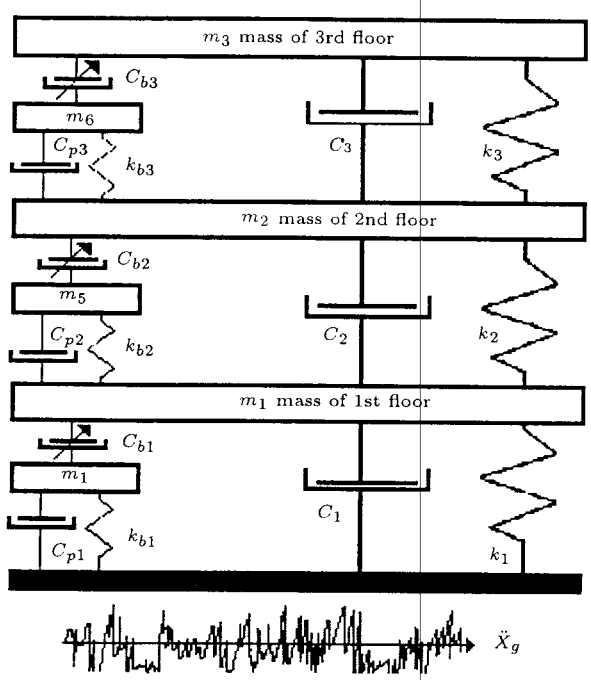

Figure 4. Finite element model.

where $\mathbf{M}$, $\mathbf{C}_p$, $\mathbf{C}_b(t)$ and $\mathbf{k}$ are mass, proportional Rayleigh damping, nonclassical damping and stiffness matrices, respectively. $\mathbf{x}$ and its derivatives are relative displacement, velocity and acceleration vectors and x_g is ground motion displacement applied at the foundation. $\mathbf{r}_g$ is a location vector to show the extent and distribution of excitation on each DOF.

Through rearranging the equation by transferring internal nonclassical damping forces to the rhs, new external forces will appear:

$$\mathbf{M}\ddot{\mathbf{x}} + \mathbf{C}_p\dot{\mathbf{x}} + \mathbf{k}\mathbf{x} = -\mathbf{M}\mathbf{r}_g\ddot{x}_g(t) - \mathbf{C}_b(t)\dot{\mathbf{x}}. \qquad (2)$$

The last term of the above equation may be interpreted as a virtual control input vector:

$$\mathbf{R}_c\mathbf{f}_c(t) = -\mathbf{C}_b(t)\dot{\mathbf{x}}, \qquad (3)$$

where $\mathbf{f}_c(t)$ is the virtual control force vector and $\mathbf{R}_c$ is a location matrix. One may imagine that instead of having internal forces in the structural system produced by dissipating energy mechanism, there are some virtual actuators that are able to apply external forces to the structure. Therefore, this semi-active control problem may be converted to a conventional active control design using, for example, adaptive control strategies. Adaptive feedforward control has been selected due to nonstationarity of the disturbance process and the quick response of feedforward controllers compared to feedback ones. However, it is noted that mathematically, an adaptive feedforward controller is equivalent to a nonadaptive feedback compensator [14,15].

For the development that follows state-space time domain and backward-shift operator calculus, q^{-1} or delay operator (or inversely, forward-shift operator q^{+1} or prediction operator) in discrete-time are used as two descriptions of dynamic systems [16-18]. If $f(k)$ is a digital sequence, in which $t_k = kT_s$, and T_s is the sampling period for converting a continuous-time signal $f(t_k)$ to the digital sequence $f(k)$, then the one-sided z-transform (or if someone misuses terminology, almost equivalently q-transform) of the signal $f(k)$ is defined by [17]:

$$F(z) \equiv \sum_{k=0}^{\infty} f(k)z^{-k}. \qquad (4)$$

The z and q variables are not exactly the same. In many system theory textbooks, z is used for the shift operator (i.e., instead of q) as well as for the complex variable in the z-transform. However, it is convenient to have different notations of the two notions. This is the same separation that is normally done between the complex variable s in the Laplace transform and the differential operator $p = d/dt$ [18,19]. Shift operator q in discrete-time is the counterpart of the differential

operator p in continuous-time. The backward-shift operator (backward in time) has the following important property [18]:

$$q^{-1}f(k) = f(k-1). \tag{5}$$

It means that the backward-shift operator causes one sampling time delay in digital sequence. The goal of backward-shift operator and algebraic system theory is to convert manipulations of difference equations to purely algebraic problems [19]. This is similar to the objective of Laplace transform operators in continuous-time processing of differential equations. The continuous-time state-variable vector of the structural system is defined by:

$$\mathbf{z} = [\mathbf{x}^T \ \dot{\mathbf{x}}^T]^T. \tag{6}$$

First-order structural dynamics equations are written in the form:

$$\dot{\mathbf{z}} = \begin{bmatrix} \mathbf{0}_{n\times n} & \mathbf{I}_{n\times n} \\ -\mathbf{M}^{-1}\mathbf{k} & -\mathbf{M}^{-1}\mathbf{C}_p \end{bmatrix} \mathbf{z} + \begin{bmatrix} \mathbf{0}_{n\times 1} \\ \mathbf{r}_g \end{bmatrix} \ddot{x}_g(t) + \begin{bmatrix} \mathbf{0}_{n\times 3} \\ \mathbf{M}^{-1}\mathbf{R}_c \end{bmatrix} \mathbf{f}_c(t) + \begin{bmatrix} \mathbf{0}_{n\times 3} \\ \mathbf{R}_n \end{bmatrix} \omega(t), \tag{7}$$

or more compactly as:

$$\dot{\mathbf{z}} = \mathbf{A}\mathbf{z} + \mathbf{b}_g\ddot{x}_g(t) + \mathbf{B}_c\mathbf{f}_c(t) + \mathbf{E}\omega(t). \tag{8}$$

This equation defines a dynamic system under a random seismic excitation and three control actions. A white noise excitation $\omega(t)$ has been added into the system, in order to incorporate local structural nonlinearities, actuator dynamics and other unmodeled dynamics indirectly [20]. When there is zero information about a random process, the easiest way for its modeling is the white noise process which has a flat power spectral density for all frequencies. In computer simulations, its intensity is determined in such a way that it can represent minor unmodeled dynamics. If this noise intensity does not cause a large deviation in the mathematically modeled dynamics of the system, adaptive filters (with adjustable parameters) are able to compensate for it. This is one of the major reasons for the superiority of adaptive filters over fixed parameter filters in unknown or poorly known environments and systems. In experimental simulations, this white noise intensity can be estimated through measured data. For simplicity of discussion, assume that input white noise excitation, implemented for modeling the unmodeled dynamics of the system, influences the structure in the same way as ground acceleration does. Thus, Equation 8 may be rewritten as follows:

$$\dot{\mathbf{z}} = \mathbf{A}\mathbf{z} + \mathbf{b}_g\ddot{x}_g(t) + \mathbf{B}_c\mathbf{f}_c(t) + \mathbf{b}_g\omega(t).$$

The above linear time-invariant continuous-time system is discretized to a linear discrete-time dynamical system by finite differences, assuming a zero-order hold [17]:

$$\mathbf{z}(k+1) = \Phi\mathbf{z}(k) + \Gamma_g\ddot{x}_g(k) + \Psi_c\mathbf{f}_c(k) + \Gamma_g\omega(k).$$

Assume that input white noise excitation and ground acceleration processes are mutually uncorrelated (possibly nonstationary) jointly Gaussian white noise sequences with the following covariance matrices:

$$\mathbf{E}\{\omega(i)\omega^T(j)\} = \mathbf{R}(i)\delta_{ij},$$

$$\mathbf{E}\{\ddot{x}_g(i)\ddot{x}_g^T(j)\} = \mathbf{Q}(i)\delta_{ij},$$

$$\mathbf{E}\{\omega(i)\ddot{x}_g^T(j)\} = \mathbf{S} = \mathbf{0}, \quad \text{for all } i \text{ and } j.$$

For this single-channel noise and ground acceleration, the covariance matrices are degenerated to variance scalars $q(i)$ and $r(i)$. A signal-to-noise ratio is defined as:

$$SNR = \frac{q(i)}{r(i)}.$$

For the case study used in this paper, SNR, approximately equal to 20, has been implemented. For a numerical study, it is assumed that all random processes are ergodic. Therefore, someone may not distinguish between ensemble and time averaging. A normally distributed random number generator, like that used by MATLAB software, may be initiated for generating the input white noise excitation with the desired variance.

As shown in Figure 5, three structural sensors for three floors and an array of ground sensors near the foundation of the structure, known as geophones, have been installed. For each story, one adaptive filter/controller, corresponding to one Λ-bracing, has been implemented.

The continuous and its discretized output measurement equations for the structural sensors are:

$$\mathbf{Y}(t) = \mathbf{C}\mathbf{z}(t) + \mathbf{d}\ddot{x}_g(t) + \mathbf{V}(t),$$

$$\mathbf{Y}(k+1) = \mathbf{C}\mathbf{z}(k+1) + \mathbf{d}\ddot{x}_g(k+1) + \mathbf{V}(k+1). \tag{9}$$

$\mathbf{Y}(t)$ is the vector of structural responses that should be controlled, $\mathbf{d}$ is the influence coefficient of earthquake disturbance, which is a zero vector in this case (but not where one is dealing with soil-structure interaction effects) and $\mathbf{V}(t)$ is the measurement noise vector that also can incorporate the echo effects from structural response to ground motion [21,22].

As an example, if the objective is controlling the base shear, $\mathbf{C}$ may be defined by:

$$\mathbf{C} = [\mathbf{k} \ \mathbf{C}_p + \mathbf{C}_b(t)]. \tag{10}$$

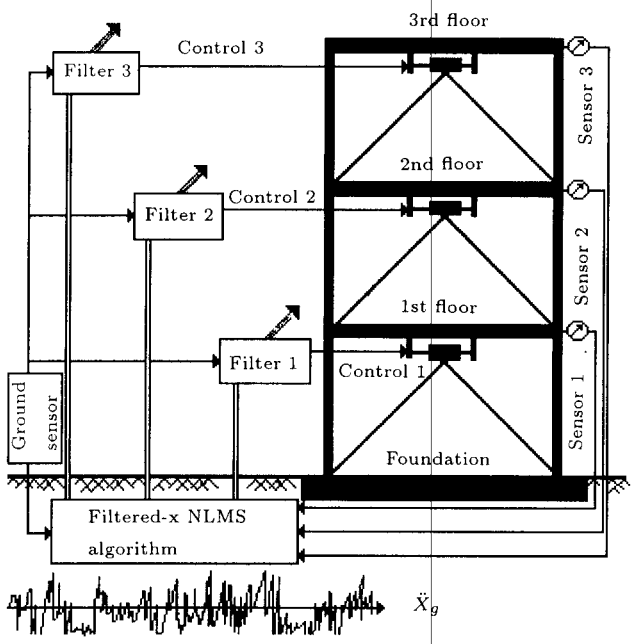

Figure 5. Complete dynamic system.

Due to the linearity assumption for the structure dynamics, error signal at discrete time k, measured at ith floor, is defined as a superposition of structural floor responses to seismic disturbance and to three control inputs [8,15,23]:

$$e_i(k) = d_i(k) + \sum_{m=1}^{3} y_{im}(k), \quad i = 1,2,3, \tag{11}$$

where digital sequences have been used for the sampling time t_k. $d_i(k)$ is the structural response due to seismic disturbance and y_{im} is the ith floor structural response to mth floor control action, as shown in Figure 6, for second floor in the block diagram schematic.

Since q-transform (or equivalently z-transform) is a linear mapping of time series into a complex-variable

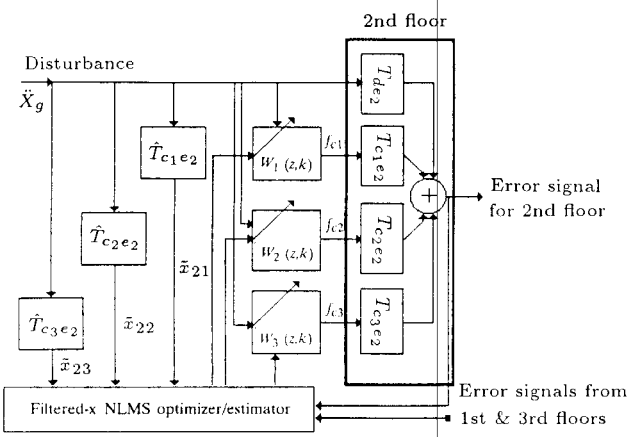

Figure 6. A block diagram for 2nd floor.

function of q, there is an equivalent relation for q-transformed error signal in the q-domain [18,19]:

$$E_i(q) = D_i(q) + \sum_{m=1}^{3} Y_{im}(q) \quad i = 1,2,3. \tag{12}$$

The following pulse-transfer functions in backward-shift operator relate the parts of error signal output to the corresponding inputs. $T_{dei}(q)$ is the pulse-transfer function from the seismic disturbance input to a part of the error signal i:

$$d_i(k) = T_{de_i}(q)\ddot{x}_g(k), \quad i = 1,2,3. \tag{13}$$

This function is actually a complex-valued rational function whose numerator and denominator are polynomials of different powers of q^{-1}. Also, $T_{cmei}(q)$ is the pulse-transfer function from the control action applied at the mth floor to the other part of the error signal i:

$$y_{im}(k) = T_{c_me_i}(q)f_{c_m}(k), \quad i = 1,2,3, \quad m = 1,2,3. \tag{14}$$

Consider the input-output relations between the control forces, as the outputs of the adaptive filters $W_m(z,k)$, and seismic disturbance input:

$$f_{c_m}(k) = W_m(q,k)\ddot{x}_g(k) \quad m = 1,2,3. \tag{15}$$

Both q and k are used as arguments of $W_m(q,k)$ controller filters to emphasize time-varying behavior of adaptive algorithms.

For comparison, the above equation in the z-domain (or loosely q^{-1}-domain) is equivalent to the following convolution sum in the time-domain:

$$f_{c_m}(k) = \sum_{j=0}^{L_m} w_m(j,k)\ddot{x}_g(k-j), \quad m = 1,2,3. \tag{16}$$

In the above equation, $w_m(j,k) = w_{mj}(k)$ is the jth weight of discrete-pulse response of mth floor adaptive filter, determined for the sampling period k. The objective in adaptive control is to calculate $W_m(q,k)$ filter weights optimally, i.e., w_{mj} at each time step k.

The relation of $W_m(q,k)$, the adaptive controller installed at mth floor, and its jth Markov parameter, $w_m(j,k)$ (or jth weight of discrete pulse response of that filter) in the q-domain is written as:

$$W_m(q,k) = \sum_{j=0}^{L_m} w_{mj}(k)q^{-j}, \quad m = 1,2,3. \tag{17}$$

$W_m(q,k)$ is an FIR (Finite Impulse Response) filter [24] that can be truncated after L_m time points for the mth floor adaptive controller that is a finite energy

stable filter. The number of parameters of the FIR filters implies that the dimension of optimization space is $(L_1+1)\times(L_2+1)\times(L_3+1)$. w_{mj}'s, at each sampling time k are the design variables [21-23]. For three semi-active dampers and $L_1 = L_2 = L_3 = 24$, this dimension is 75.

By substituting Equations 15 and 17 into Equation 14, the following relation is obtained:

$$y_{im}(k) = T_{c_m e_i}(q) \sum_{j=0}^{L_m} w_{mj}(k) q^{-j} \ddot{x}_g(k),$$

$$i, m = 1, 2, 3. \tag{18}$$

Substituting from Equations 13 and 18 into Equation 11, the error signal is obtained in terms of structural transfer functions:

$$e_i(k) = T_{de_i}(q)\ddot{x}_g(k) + \sum_{m=1}^{3} T_{c_m e_i}(q) \sum_{j=0}^{L_m} w_{mj}(k) q^{-j} \ddot{x}_g(k),$$

$$i = 1, 2, 3. \tag{19}$$

A filtered sequence of acceleration seismic signal through structural transfer functions is defined by:

$$\ddot{\tilde{x}}_{mi}(k) = T_{c_m e_i}(q)\ddot{x}_g(k), \quad m, i = 1, 2, 3. \tag{20}$$

This filtered signal contains only those poles that may cause strong resonance to the structural system. By this signal, only those poles of acceleration seismic signal that are able to excite the system, are entered into the identification process of LMS algorithm during the optimization of the filter weights. The other less important poles of actual seismic signal are filtered out. This is the core idea of the filtered version of LMS algorithm.

Substituting the filtered seismic signal (Equation 20) into the error signal (Equation 19), the following relation is obtained:

$$e_i(k) = T_{de_i}(q)\ddot{x}_g(k) + \sum_{m=1}^{3} \sum_{j=0}^{L_m} w_{mj}(k) \ddot{\tilde{x}}_{mi}(k-j),$$

$$i = 1, 2, 3. \tag{21}$$

The above relation has been written by the use of backward-shift operator property:

$$q^{-j} \ddot{\tilde{x}}_{mi}(k) = \ddot{\tilde{x}}_{mi}(k-j). \tag{22}$$

The mean squares of error signals are chosen as a quadratic convex objective function for determining the optimal values of $w_{mj}(k)$, Markov parameters of the $W_m(q,k)$ filter at time k:

$$C\left(w_{mj}(k)\right) = \sum_{i=1}^{3} \mathbf{E}\{\mathbf{e}_i^2(k)\},$$

$$j = 0, ..., L_m \quad m = 1, 2, 3. \tag{23}$$

$\mathbf{E}\{.\}$ is a notation for the statistical expectation operator. Clearly, this function has only one global minimum and, hence, the solution is unique. The easiest technique to find that minimum is the steepest descent method and searching for the updated values of filter weights in the negative of gradient, while the search step size should guarantee the stability of the algorithm [21,22].

Through calculating the gradient of the cost function (Equation 23) relative to the adaptive filter coefficients, it is obtained that:

$$\frac{\partial C(w_{mj}(k))}{\partial w_{mj}(k)} = \sum_{i=1}^{3} \mathbf{E}\left\{2\mathbf{e}_i(k) \frac{\partial e_i(k)}{\partial w_{mj}(k)}\right\},$$

$$i = 1, 2, 3, \quad m = 1, 2, 3. \tag{24}$$

The approximation of this deterministic gradient converging theoretically to Wiener filter solution, by a stochastic gradient, yields the so-called Least Mean Square (LMS) algorithm:

$$\frac{\partial C\left(w_{mj}(k)\right)}{\partial w_{mj}(k)} \cong \sum_{i=1}^{3} 2e_i(k) \frac{\partial e_i(k)}{\partial w_{mj}(k)}. \tag{25}$$

Using this gradient, the general recursive updating formula of steepest descent, given by:

$$w_{mj}(k+1) = w_{mj}(k) - \gamma \frac{\partial C(w_{mj}(k))}{\partial w_{mj}(k)}, \tag{26}$$

is specialized to the following difference equation for filter weights update in LMS algorithm:

$$w_{mj}(k+1) = w_{mj}(k) - 2\gamma \sum_{i=1}^{3} e_i(k) \frac{\partial e_i(k)}{\partial w_{mj}(k)}. \tag{27}$$

Gradient of error signal relative to filter weight vector is called sensitivity derivative in adaptive control literature. The multiplication shows inherent nonlinearity of adaptive controllers. The sensitivity derivatives are calculated by differentiating error signals in Equation 21:

$$\frac{\partial e_i(k)}{\partial w_{mj}(k)} = \ddot{\tilde{x}}_{mi}(k-j),$$

$$m, i = 1, 2, 3, \quad j = 0, ..., L_m. \tag{28}$$

The final result of the filtered-x LMS algorithm is:

$$w_{mj}(k+1) = w_{mj}(k) - 2\gamma \sum_{i=1}^{3} e_i(k)\ddot{\tilde{x}}_{mi}(k-j),$$

$$m,i = 1,2,3, \quad j = 0,...L_m. \tag{29}$$

It is observed that, nine filtered-x seismic signals and, therefore, nine transfer functions $T_{cmei}(q)$ should be estimated for this multivariable control strategy. It should be noted that the derivation of classical LMS algorithm is the same as above, except that the filtered-x seismic signals are replaced by (nonfiltered) seismic input signals. Referring to the block diagram of Figure 6, in classical LMS algorithm there is no need for filtering seismic disturbances through the estimated (overhat) structural transfer functions, as shown in that diagram. The major difficulty of filtered-x version of LMS algorithm is to estimate structural transfer functions $T_{cmei}(q)$ for obtaining filtered seismic signals. However, this can be accomplished by having a rough finite element model of the structure:

$$\ddot{\tilde{x}}_{mi}(k) \cong \hat{T}_{c_m e_i}(q)\ddot{x}_g(k), \quad m,i = 1,2,3\ , \tag{30}$$

where overhat, $T_{c_m e_i}(q)$, has been calculated from the finite element model.

For the purpose of comparison, the derivation of the Single-Input Single-Output version of filtered-x LMS algorithm has been presented in Appendix 1.

The SISO derivation using the z-transform concept for active control is due to [11]. The Two-Input Two-Output derivation using z-transform for active control is due to [9,12]. The single channel and multichannel derivations using convolution and matrix representation for active control have been presented by [25,26]. The Three-Input Three-Output derivation using Backward-shift operator in time (delay operator or q^{-1}-Calculus), for semi-active control is due to these authors.

CONTROL RULE FOR SEMI-ACTIVE FILTER

Up to this point, the assumptions have been compatible with the conventional active controllers that consume a large amount of external energy and that need a large power supply. However, it is remembered from Equation 3 that by designing $f_c(t)$, one may actually find some optimal values for $\mathbf{C}_b(t)$, the nonclassical damping matrix of energy dissipating systems. Equations 7 and 8 are expanded in order to see the facts more clearly:

$$\dot{\mathbf{z}} = \mathbf{A}\mathbf{z} + \mathbf{b}_g\ddot{x}_g(t) + \sum_{m=1}^{3} \mathbf{b}_{c_m} f_{c_m}(t) + \mathbf{E}\omega(t)$$

$$m = 1,2,3 \tag{31}$$

$$y_m = \mathbf{C}_m\mathbf{z} + d_m\ddot{x}_g(t) + V_m(t),$$

$$\mathbf{Y} = [y_1, y_2, y_3]^T \tag{32}$$

It is clear from Equations 3,7,8 and 31 that:

$$r_{c_m} f_{c_m}(t) = -\mathbf{C}_{b_m}(t)\dot{\mathbf{x}}_m, \quad m = 1,2,3\ , \tag{33}$$

where matrices $\mathbf{R}_c$ and $\mathbf{C}_b(t)$ have been partitioned to corresponding vectors $\mathbf{r}_{cm}$ and matrices $\mathbf{C}_{bm}(t)$. Consequently, the following scalar equation is obtained:

$$f_{c_m}(t) = \bar{C}_{b_m}(t)[\dot{x}_m - \dot{x}_{m+n}], \quad m = 1,2,3. \tag{34}$$

The index n is the total number of energy dissipating systems and overbar $C_{bm}(t)$ is a measure of the damping coefficient of that system. It is clear from stability reasons that:

$$\bar{C}_{b_m}(t) = \left| \frac{f_{c_m}(t)}{\dot{x}_m(t) - \dot{x}_{m+n}(t)} \right|$$

$$m = 1,2,3, \quad \dot{x}_m - \dot{x}_{m+n} \neq 0 \tag{35}$$

Due to practical constraints, the overbar C_{bm} variations have been limited between two upper and lower practical limits:

$$\bar{C}_{\text{lower}} \leq \bar{C}_{b_m}(t) \leq \bar{C}_{\text{upper}} \quad \forall t. \tag{36}$$

In this way, actually, a parametrically excited nonlinear vibration problem is running, in which the sources of the parametric excitations are the internal change of dynamic characteristics of the system.

THE OBJECTIVE FUNCTIONS

In adaptive filtering and control literature, the "desired response" or "training signal" is the signal that should be followed by the output of the adaptive filters. The parameters of the adaptive filters are adjusted to cause their output resultant to agree as closely as possible with the desired response signal. This is accomplished by comparing this output resultant with the desired response to obtain an "error signal" and then adjusting or optimizing the parameters to minimize this signal [22]. In general, the desired response is simply some objective output that the adaptive filter must be designed to replicate in opposite phase [15].

In adaptive feedforward control of seismically-excited structures, the desired response or training signal is any response of the uncontrolled structure (to seismic signal) that the designer wishes to be minimized. The uncontrolled structure means the primary structure without any augmented active or semi-active control system. The output resultant of adaptive filters is the resultant response of the structure

to the active or semi-active control systems when the response to the seismic excitation is off. The error signal is the linear superposition of these two principal effects on the structure under control.

There is some degree of freedom in the definition of the kind of a desired response or objective response. In this project, three different objectives have been implemented and the results have been compared:

1. The Relative Floor Displacement vector with the structural stiffness matrix as a weighting matrix (RFD objective response). By this definition, an effort is made to minimize the elastic potential energy of the system. For this case, $T_{dei}(q)$ are the Structural Transfer Functions (STF) from seismic acceleration to the RFD's.
2. The Total Base Shear in the first story columns and bracing systems (TBS objective response). For this case, $T_{de}(q)$ is the STF from seismic acceleration to the TBS at the ground floor level.
3. The Column Base Shear, i.e., the base shear only in the first story columns (CBS objective response). It is assumed that the construction method allows the first story bracing to convey its load directly to the foundation. For this case, $T_{de}(q)$ is the STF from seismic acceleration to the CBS at ground floor level.

NUMERICAL RESULTS AND DISCUSSION

In numerical simulation, El Centro, 1940 earthquake has been applied to the 3-story flexible structure, for a 20 second period. Its first six natural frequencies and modal proportional damping properties are given in Table 1. This structure has been equipped with three energy dissipation mechanism attached to bracing systems. There are two simulations performed with this structure. The first simulation is called passive uncontrolled, because during the simulation, the damper coefficients of the energy dissipation systems are kept fixed. In fact, this case is equivalent to a passive system. The second simulation is called controlled, because the damper coefficients are adjusted continuously between two practical limits.

The simulation results have been obtained by MATLAB^{TM}. Relative displacements and drifts between floors have been normalized relative to the maximum absolute value of the third floor relative displacement of uncontrolled structure; floor absolute accelerations relative to gravity and force responses relative to the building weight. Numerical values of maximum and minimum controlled responses are marked by dotted horizontal straight lines in the graphs; while upper and lower limits of each graph have been set for maximum and minimum values of uncontrolled responses. RRF (Response Reduction Factor) needs to be defined. It is the relative reduction percent of response between uncontrolled and controlled systems.

Table 1. Dynamic properties of simulated structure.

Mode	Frequency (Hz)	Damping (%)
1	0.5000	1.0000
2	1.1438	2.0000
3	1.4649	3.0000
4	2.1240	4.0000
5	2.4528	5.0000
6	2.6296	6.0000

A brief comment and discussion are presented on the figures and tables. Only the responses obtained considering the TBS objective response algorithm are shown in the figures.

Figure 7 is the third floor displacement relative to the foundation. From Tables 2a, 3a and 4a, it is observed that the CBS algorithm has been the most effective method among these three objective response algorithms, for reducing floor displacements with an average RRF of 59.09%. The TBS algorithm is the most inefficient algorithm among the three, with an average RRF of 56.88%.

Figure 8 demonstrates the drift between the second and first floors. The TBS objective response algorithm has reduced the drift responses more than the other two algorithms. It seems that the RFD algorithm is the least efficient method for this kind of response. It should be pointed out that there are no critical differences between the performance of these three objective algorithms. Figures 9 and 10 show the total and column base shear time histories that have been chosen as the criteria for the TBS and CBS algorithms, respectively. The total base shear is the shear due to both column and bracing actions, but the column base shear is due to only the column action. It is clear that the optimization algorithms based on the base shear forces have tried to reduce the related base

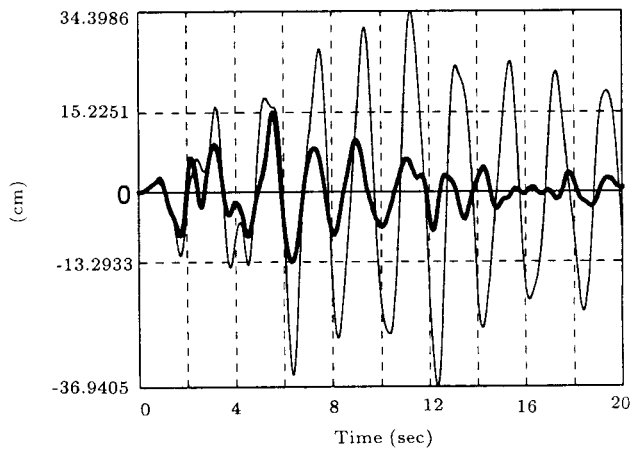

Figure 7. 3rd floor relative displacement.

Table 2a. Calculation of RRF for major responses. Objective criterion based on TBS.

Floor No.	Max Floor Displacements			Max Cumulative Shears (%)			Max Abs. Accelerations (%g)		
	Controlled	Uncontrolled	RRF	Controlled	Uncontrolled	RRF	Controlled	Uncontrolled	RRF
3	15.23	36.94	58.78	6.94	11.78	41.09	34.11	66.80	48.94
2	30.86	74.74	58.71	10.11	17.10	40.90	18.26	33.55	45.56
1	17.93	38.28	53.16	12.64	21.47	41.13	25.84	34.84	25.84
Average RRF			56.88			41.04			40.11

Table 2b. Additional calculated responses and energy comparison.

Max Drift b/w 3rd & 2nd Floors(%)			Max Potential Energy (kJ)			Max PE+kE Energy (kJ)		
Controlled	Uncontrolled	RRF	Controlled	Uncontrolled	RRF	Controlled	Uncontrolled	RRF
11.43	39.84	71.32	7.19	32.30	77.74	12.20	50.72	75.94
Max Drift b/w 2nd & 1st Floors (%)			Max Kinetic Energy (kJ)			Max Column Base Shear (%)		
Controlled	Uncontrolled	RRF	Controlled	Uncontrolled	RRF	Controlled	Uncontrolled	RRF
14.79	43.22	65.77	10.55	47.64	77.85	10.01	21.41	53.23
Average RRF		68.55			77.80			

Table 3a. Calculation of RRF for major responses. Objective criterion based on CBS.

Floor No.	Max Floor Displacements			Max Cumulative Shears (%)			Max Abs. Accelerations (%g)		
	Controlled	Uncontrolled	RRF	Controlled	Uncontrolled	RRF	Controlled	Uncontrolled	RRF
3	14.77	36.94	60.02	7.27	11.78	38.28	37.96	66.80	43.18
2	29.29	74.74	60.81	10.23	17.10	40.21	19.10	33.55	43.07
1	16.67	38.28	56.45	13.89	21.47	35.29	26.21	34.84	24.79
Average RRF			59.09			37.93			37.01

Table 3b. Additional calculated responses and energy comparison.

Max Drift b/w 3rd & 2nd Floors(%)			Max Potential Energy (kJ)			Max PE+KE Energy (kJ)		
Controlled	Uncontrolled	RRF	Controlled	Uncontrolled	RRF	Controlled	Uncontrolled	RRF
11.45	39.84	71.26	6.93	32.30	78.54	12.25	50.72	75.84
Max Drift b/w 2nd & 1st Floors (%)			Max Kinetic Energy (kJ)			Max Column Base Shear (%)		
Controlled	Uncontrolled	RRF	Controlled	Uncontrolled	RRF	Controlled	Uncontrolled	RRF
15.10	43.22	65.06	10.81	47.64	77.32	9.32	21.41	56.48
Average RRF		68.16			77.93			

Table 4a. Calculation of RRF for major responses. Objective criterion based on RFD.

Floor No.	Max Floor Displacements			Max Cumulative Shears (%)			Max Abs. Accelerations (%g)		
	Controlled	Uncontrolled	RRF	Controlled	Uncontrolled	RRF	Controlled	Uncontrolled	RRF
3	15.25	36.94	58.71	6.79	11.78	42.33	31.99	66.80	52.11
2	29.88	74.74	60.02	10.34	17.10	39.52	16.70	33.55	50.21
1	16.04	38.28	58.10	13.41	21.47	37.53	25.71	34.84	26.23
Average RRF			58.94			39.79			42.85

Table 4b. Additional calculated responses and energy comparison.

Max Drift b/w 3rd & 2nd Floors(%)			Max Potential Energy (kJ)			Max PE+KE Energy (kJ)		
Controlled	Uncontrolled	RRF	Controlled	Uncontrolled	RRF	Controlled	Uncontrolled	RRF
11.92	39.84	70.08	6.93	32.30	78.56	12.29	50.72	75.76
Max Drift b/w 2nd & 1st Floors (%)			Max Kinetic Energy (kJ)			Max Column Base Shear (%)		
Controlled	Uncontrolled	RRF	Controlled	Uncontrolled	RRF	Controlled	Uncontrolled	RRF
15.22	43.22	64.78	10.82	47.64	77.28	8.96	21.41	58.16
Average RRF		67.43			77.92			

shears. However, from a simple averaging consideration for this specific simulation, it seems that the RFD and TBS algorithms have performed better than the CBS algorithm.

Figure 11 shows the third floor absolute acceleration response. The RFD and, then, TBS algorithms have reduced this kind of response more than the CBS algorithm.

Figure 12 shows the first floor damping force time history. It is observed that for some time, the damping force has been about 8% of the building weight for a controlled system. In comparison with the large amplitude damping force of the controlled system, the damping force time history of the uncontrolled system can hardly be seen from the figure.

Figures 13 and 14 illustrate the force-displacement curves. The force is the total base shear and the displacement is the drift between the first floor and the foundation. The hysteresis loops for the controlled structure are much wider than those for the uncontrolled structure. It may be observed how large a damping force would be developed in a controlled structure, as compared to an uncontrolled one.

Figure 15 shows the amount of external energy injected from the acceleration seismic signal input to the controlled and uncontrolled structures. The seismic input energy is more for the uncontrolled structure.

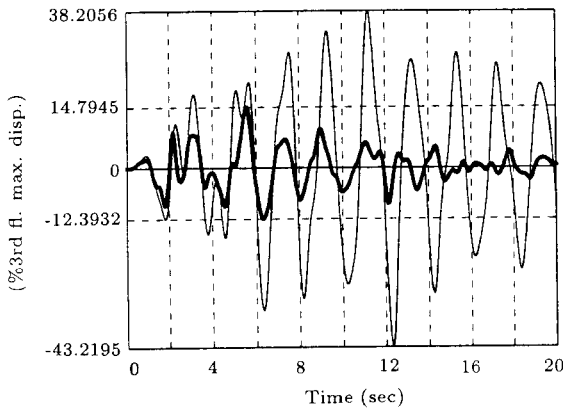

Figure 8. Drift b/w 2nd and 1st floors.

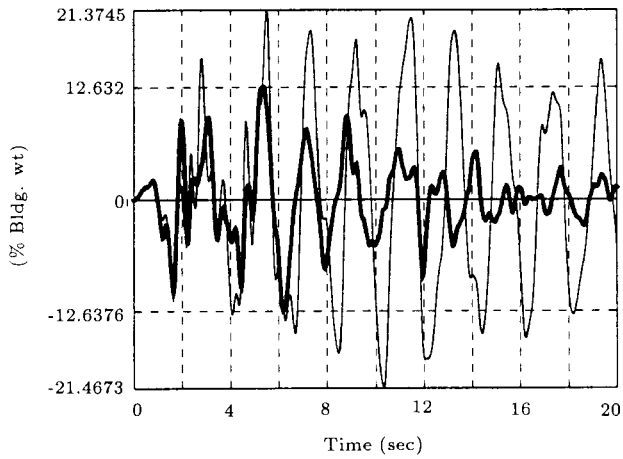

Figure 9. Total base shear force.

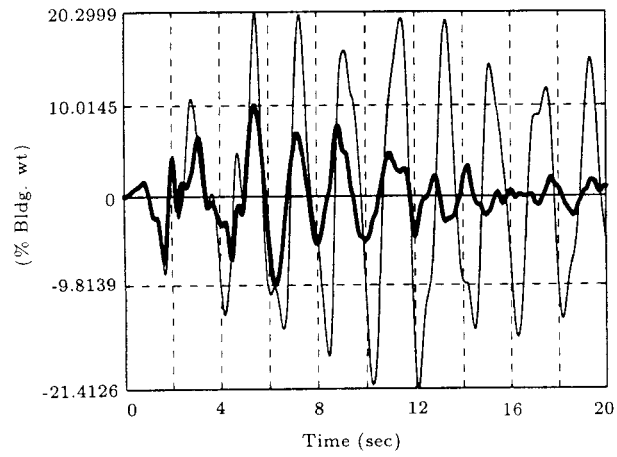

Figure 10. Column base shear force.

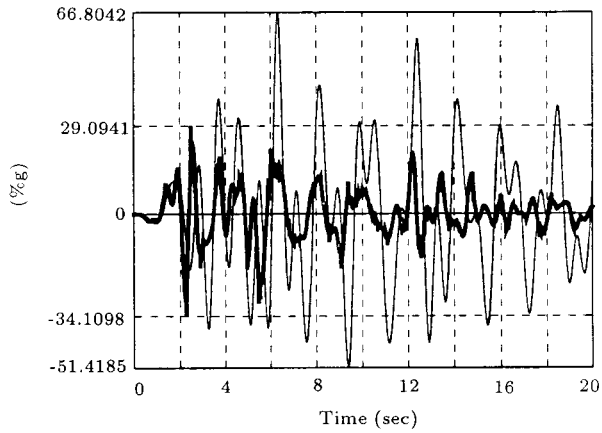

Figure 11. 3rd floor absolute acceleration.

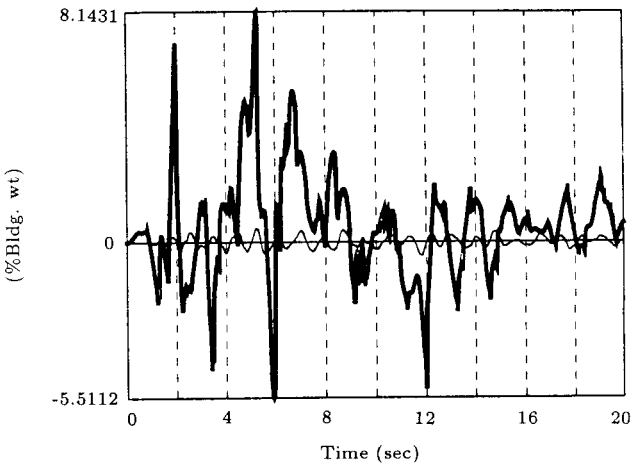

Figure 12. 1st floor damping force.

Also, it is observed from Figure 16 that the absorbed dynamical energy (potential+kinetic) is greater for the uncontrolled structure. The reason is that much more energy has been damped out in the dampers

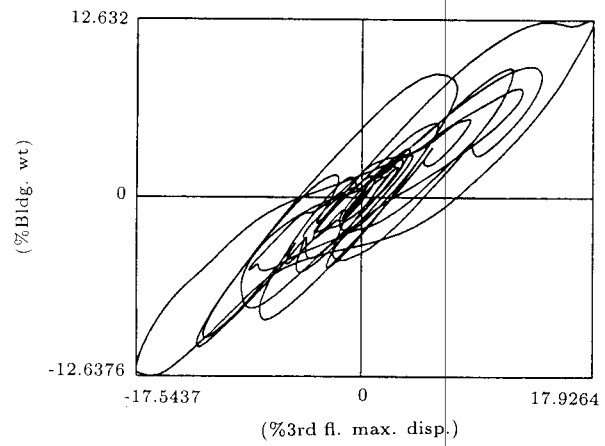

Figure 13. Base shear-1st floor displacement (controlled).

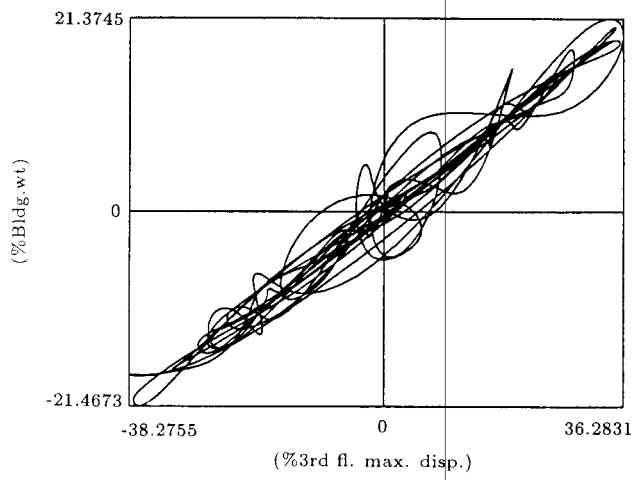

Figure 14. Base shear-1st floor displacement (uncontrolled).

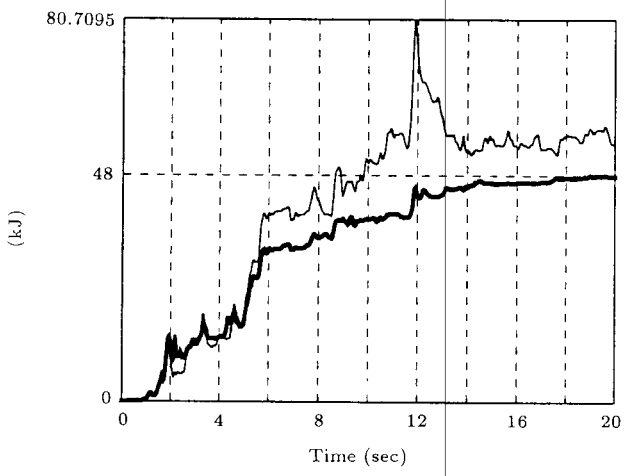

Figure 15. Earthquake input energy.

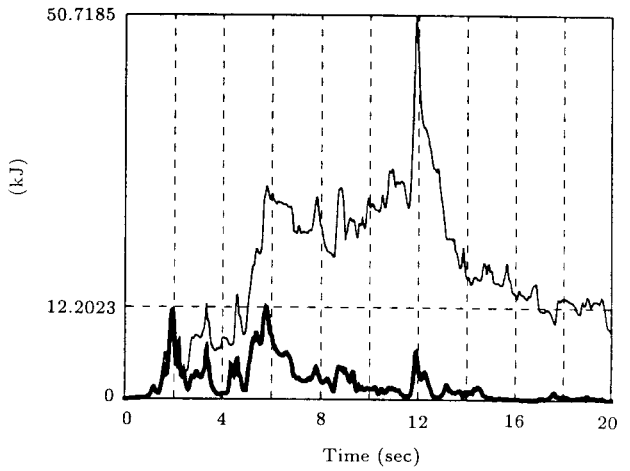

Figure 16. PE + KE stored energy.

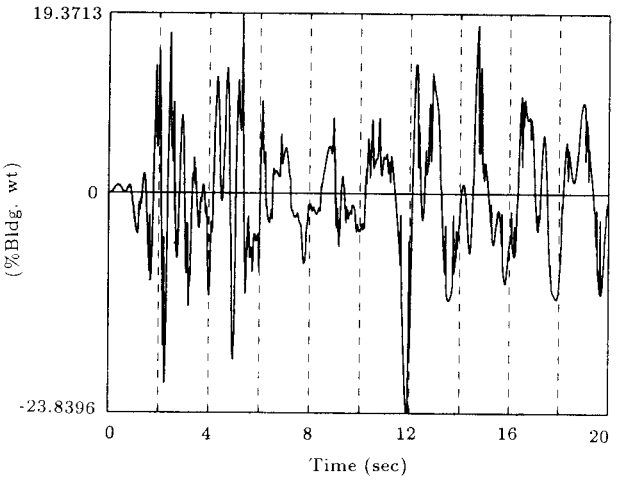

Figure 17. 1st floor virtual control force.

of the controlled structure. The maximum seismic input energy for the uncontrolled system is 80.71 kJ. The TBS algorithm has reduced this peak to 48.00 kJ, with an RRF of 40.53%. The RRFs for the RFD and CBS algorithms are 42.68% and 42.36%, respectively. Therefore, the RFD has been the most efficient algorithm among the three, for reducing the peak of seismic input energy response, as was expected.

Figure 17 shows the virtual control force obtained by LMS algorithm for the first floor virtual actuator. If the system were an active controller, then force should have been applied to the system by using some transduction devices and consuming lots of external energy. However, for this semi-active controller, these virtual control forces are divided by some relative velocities to obtain some measure for semi-active damper parameters. The variations of the resulting nonclassical damping coefficient for the variable-orifice damping device, installed at the second floor, has been drawn in Figure 18, between two practical lower and upper limits.

Figures 19 to 21 show the evolution of adaptive

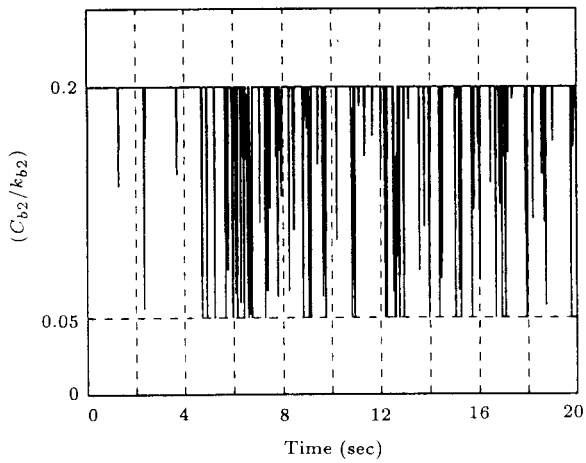

Figure 18. 2nd floor semi-active damper coefficient.

filter weights of each floor with time. The convergence for the controller installed at the third floor has been very rapid. However, for the first floor, the rate of convergence is low or even the parameters are diverging.

The graphs showing the time evolution of adaptive controller weights are directly a measure of performance of the active controller. The time evolution of the nonclassical damping coefficient of semi-active damping devices has been obtained by dividing the virtual active control forces, obtained from LMS algorithm, by the relative velocities between each floor and lower bracing. Therefore, the convergence (or divergence) of the weights may be an indirect measure of the stability, robustness and performance of the algorithm for the semi-active damper. In addition, from Figure 21, it may be deduced that it is possible to identify the dynamic characteristics of the adaptive filter installed at the third floor by fewer parameters.

Figure 22 shows the FIR parameters of the first floor adaptive filter for the 20th second after the simulation initializes. These parameters are the same as the discrete-pulse response of the adjustable filter at that time. The number of parameters for all filters has been selected to truncate after 25 sample numbers. Although the pulse response of the filter does not equal zero for the 25th parameter, the performance of the filter and the LMS algorithm has been satis-

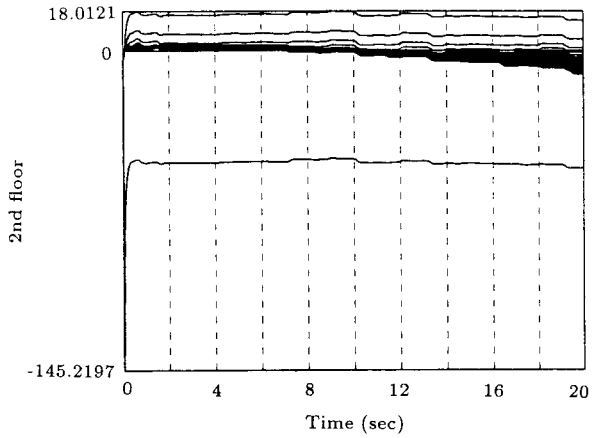

Figure 20. Adaptive controller weights for second floor.

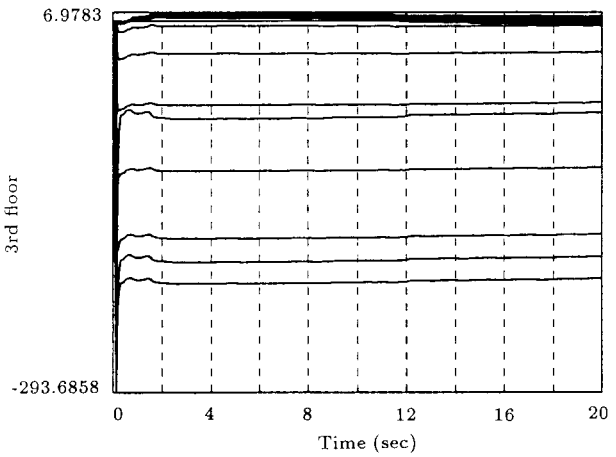

Figure 21. Adaptive controller weights for third floor.

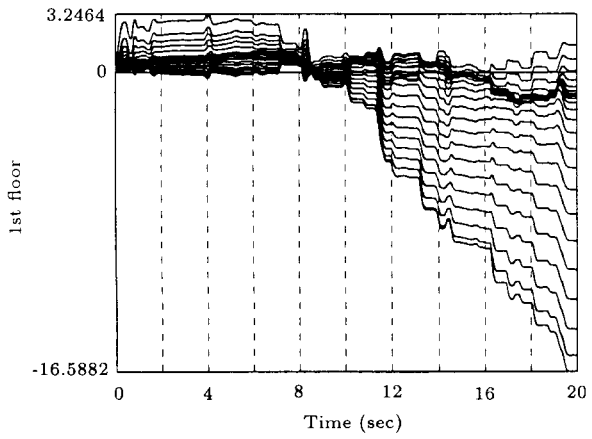

Figure 19. Adaptive controller weights for first floor.

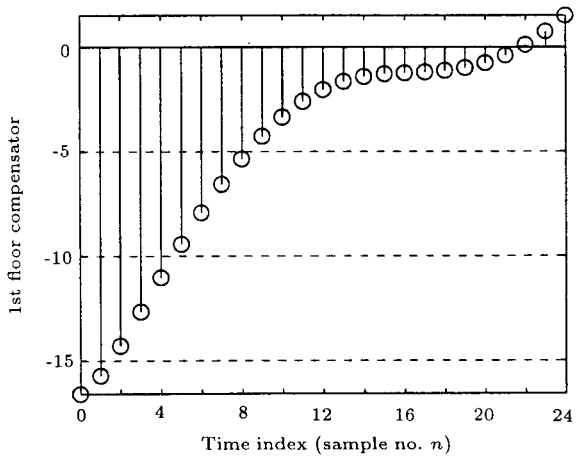

Figure 22. Discrete pulse for the 20th second.

factory. Figures 23 and 24 illustrate how semi-active damping coefficient time history may be interpreted as time evolution of orifice size in the mechanism. For the purpose of illustration, consider the hypothetical cylindrical semi-active damper with internal radius R, whose cross-sectional design is shown in Figure 24. The piston head is characterized by its radius R_p and axial length L_p. The chambers are filled with an incompressible viscous fluid obeying Newton's viscosity law and having dynamic viscosity μ and density ρ. Meanwhile, the piston rod is assumed to move in the axial direction with velocity V, forcing the fluid through the annular passage of width $h = R - R_p$ and thus producing a pressure differential across the head. Assume that an accumulator is present to compensate for the volumetric changes associated with the piston rod. There are two groups of oil intakes. The first group is designed as the annular passage around the main piston head within the cylinder for a minimum passive action available all the time. The second group is provided through by-pass passages outside the main cylinder for semi-active action, possibly by the same mechanism of annular passages around some piston heads. The time deviations of nonclassical damping coefficients are developed in these by-pass intakes. If it is assumed that there are six by-pass intakes, all having $\mu = 0.26$ kg/(m.sec), $L_{ps} = 0.5$ m and $R_{ps} = 0.1$ m, the time evolution of the annular passage width is shown in Figure 23.

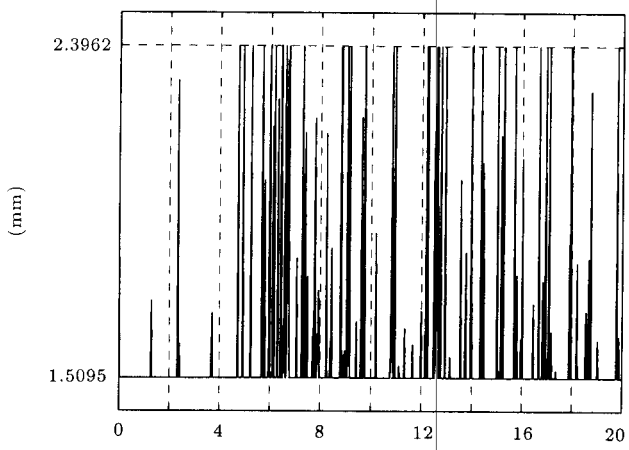

Figure 23. 2nd floor semi-active damper orifice.

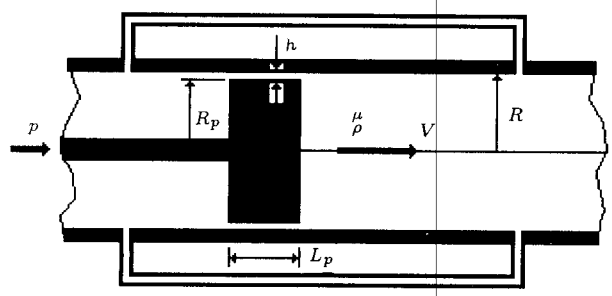

Figure 24. Hypothetical orificed fluid semi-active damper.

For this calculation, it has been assumed that $h << R$, a high viscosity fluid, small gaps, long flow passages and the Navier-Stokes equations for a planar uniaxial flow are applicable. The simplified formula is [5]:

$$C_b = 3\pi\mu L_p \left(\frac{R_p}{h}\right)^3$$

Figure 23 specifically shows the usage of the formula for this case study.

In Tables 2b, 3b and 4b, there are more responses which have been compared. As observed, the RFD algorithm has been the most effective criterion for reduction of potential energy and less effective for reduction of kinetic energy in the structure.

In the last column of each table, it may be observed that the sum of potential and kinetic energies has been reduced more by the TBS algorithm, as compared with the other two algorithms. In fact, the TBS tries to minimize both the potential and kinetic energies of the structure, indirectly. However, in the CBS and RFD algorithm minimizing potential energy is the main concern. Thus, it is the designer's choice whether more attention should be paid to the reduction of the system potential energy or the total dynamical energy.

CONCLUSIONS

In this paper, a semi-active multivariable adaptive feed-forward controller was designed for a framed structure under seismic excitations, based on filtered-x NLMS algorithm.

The hardware of the controller was an on-off orifice, viscous fluid energy dissipation mechanism, powered by a battery-size power supply that was modeled as a variable-orifice semi-active damper for numerical simulations. For each floor, one of these mechanisms was installed between that floor and the bracing system underneath.

The software of the controller was an FIR adaptive filter whose parameters were identified by the filtered-x NLMS optimizer.

The advantage of using this technology was that the need for a large power supply had been omitted. However, the numerical results showed a good performance of the dynamic compensator for the reduction of the desired structural responses.

The major results of three different optimization objective functions were summarized. These algorithms were compared for the responses of an uncontrolled passive and a controlled semi-active structure.

In summary, for this case study, it was shown that the Column Base Shear (CBS) and Relative Floor

Displacement (RFD) objective response criteria performed almost equivalently from an energy viewpoint. Both of them tried to minimize an index of potential energy. However, the Total Base Shear (TBS) objective response criterion paid more attention to minimizing total dynamical energy.

For this case study, no sharp distinction in the performance of these three criteria was observed. Each of them tried to minimize some structural responses and were efficient. It seems that for an overall response reduction, a multi-objective criterion would be more beneficial, if it does not contradict the equations of the dynamic system. These equations constitute the constraints of the optimization problem. As a whole, the results for this semi-active control strategy are encouraging and bring the hope of a near future application of this technology to special structures, like nuclear power plants.

REFERENCES

1. Nemir, D.C., Lin, Y. and Osegueda, R.A. "Semiactive motion control using variable stiffness", *ASCE J. of Str. Eng.*, **120**(4), pp 1291-1307 (1994).
2. Inman, D.J., *Vibration with Control, Measurement and Stability*, Prentice-Hall (1989).
3. Spencer, B.F. and Sain, M.K. "Controlling buildings: A new frontier in feedback", *IEEE Control Systems Mag.*, pp 19-35 (Dec. 1997).
4. Housner, G.W., Bergman, L.A., Caughey, T.K., Chassiakos, A.G., Claus, R.O., Masri, S.F., Skelton, R.E., Soong, T.T., Spencer, B.F. and Yao, J.T.P. "Structural control: Past, present, and future", *ASCE J. of Eng. Mech., Special Issue*, **123**(9), pp 897-971 (1997).
5. Soong, T.T. and Dargush, G.F., *Passive Energy Dissipation Systems in Structural Engineering*, John Wiley & Sons (1997).
6. Symans, M.D. and Constantinou, M.C. "Seismic testing of a building structure with a semi-active fluid damper control system", *Earthquake Eng. Str. Dyn.*, **26**(7), pp 759-778 (1997).
7. Meirovitch, L., *Dynamics and Control of Structures*, John Wiley & Sons (1990).
8. Skogestad, S. and Postlethwaite, I., *Multivariable Feedback Control, Analysis and Design*, John Wiley & Sons (1996).
9. Smith, J.P., Burdisso, R.A. and Suarez, L.E. "An experimental investigation of adaptive control of secondary systems", *First World Conference on Structural Control*, CA, USA (Aug. 3-5, 1994).
10. Vipperman, J.S., Burdisso, R.A. and Fuller, C.R. "Active control of broadband structural vibration using the LMS adaptive algorithm", *J. Sound and Vibration*, **166**(2), pp 283-299 (1993).
11. Burdisso, R.A., Suarez, L.E. and Fuller, C.R. "Feasibility study of adaptive control of structures under seismic excitation", *ASCE J. of Eng. Mech.*, **120**(3), pp 580-592 (1994).
12. Burdisso, R.A. "Structural attenuation due to seismic inputs with active/adaptive systems", *First World Conference on Structural Control*, CA, USA (Aug. 3-5, 1994).
13. Soong, T.T. "Active structural control, theory and practice", *Longman Scientific & Technical* (1990).
14. Fuller, C.R., Elliot, S.J. and Nelson, P.A., *Active Control of Vibration*, Academic Press (1996).
15. Clark, R.L., Saunders, W.R. and Gibbs, G.P., *Adaptive Structures*, John Wiley & Sons (1998).
16. Brogan, W.L., *Modern Control Theory*, 3rd Ed., Prentice-Hall (1991).
17. Franklin, G.F., Powell, J.D. and Workman, M.L. *Digital Control of Dynamic Systems*, Addison-Wesley (1990).
18. Astrom, K.J. and Wittenmark, B., *Computer-Controlled Systems: Theory and Design*, 2nd Ed., Prentice-Hall, NJ, USA (1990).
19. Astrom, K.J. and Wittenmark, B., *Adaptive Control*, Addison-Wesley (1988).
20. Sastry, S. and Bodson, M., *Adaptive Control, Stability, Convergence and Robustness*, Prentice-Hall Int. (1989).
21. Haykin, S., *Adaptive Filter Theory*, 3rd Ed., Prentice-Hall (1996).
22. Widrow, B. and Stearns, S.D., *Adaptive Signal Processing*, Prentice-Hall, NJ, USA (1985).
23. Slotine, J.J.E. and Li, W., *Applied Nonlinear Control*, Prentice-Hall (1991).
24. Proakis, J.G. and Manolakis, D.G., *Introduction to Digital Signal Processing*, Macmillan Pub. Co., NY, USA (1989).
25. Elliot, S.J., Stothers, I.M., and Nelson, P.A. "A Multiple error LMS algorithm and its application to the active control of sound and vibration", *IEEE Transactions on Acoustics, Speech, and Signal Processing*, **ASSP-35**(10), pp 1423-1434 (1987).
26. Kuo, S.M. and Morgan, D.R., *Active Noise Control Systems*, Wiley, NY, USA (1996).
27. Oppenheim, A.V. and Schafer, R.W., *Discrete-Time Signal Processing*, Prentice-Hall (1989).

APPENDIX

Derivation of Single-Channel Filtered-X LMS

For a comparison of formulations, the relations for the Single Input-Single Output case (SISO) is derived. Consider the structure and its block diagram (see Figures A1 and A2).

The error signal (the dynamic response that should be minimized by use of an appropriate objective function) is composed of a structural response due to:

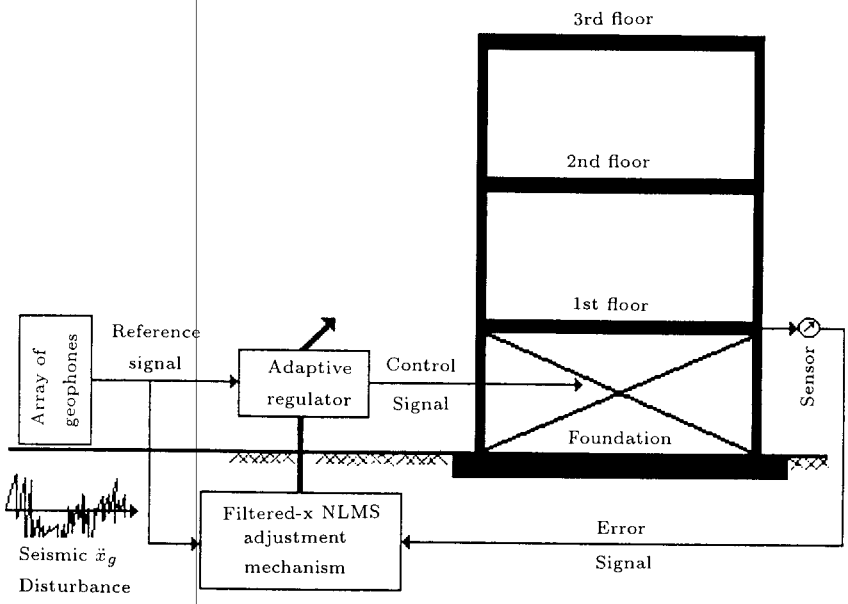

Figure A1. SISO filtered-x LMS structure-control-active dissipating system.

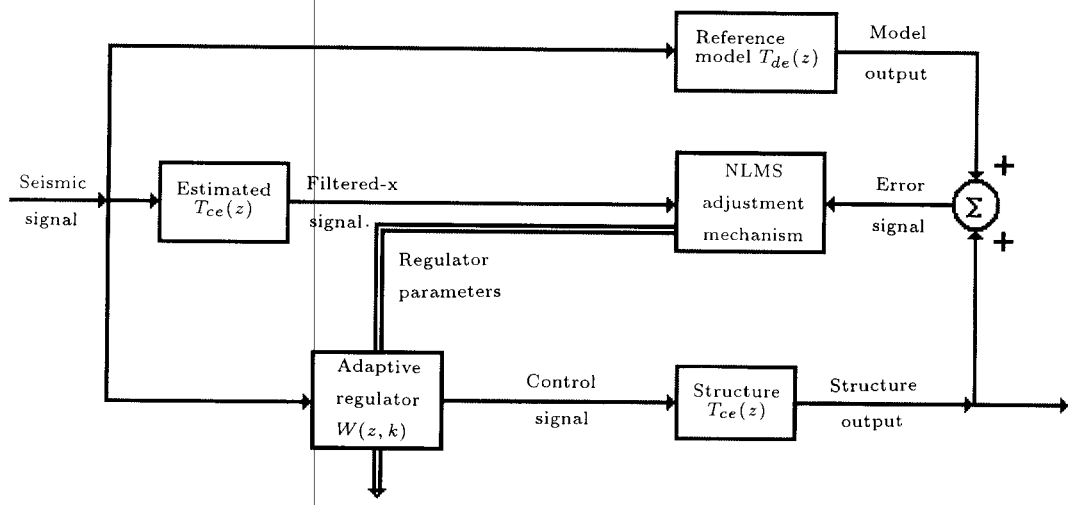

Figure A2. Block diagram equivalent of the above system.

1. A seismic disturbance as if there is no control on the structure (model output $T_{de}(z)$, that is the model of uncontrolled structure),
2. A response due to a control input (controlled structure output $T_{ce}(z)$):

$$e(k) = d(k) + y(k).$$

The following pulse-transfer functions in backward-shift operator domain are relating the parts of error signal output to the corresponding inputs. $T_{de}(q)$ is the pulse-transfer function from the seismic disturbance input to a part of the error signal:

$$d(k) = T_{de}(q)\ddot{x}_g(k).$$

This function is actually a complex-valued rational function whose numerator and denominator are polynomials of different powers of q^{-1}. In addition, $T_{ce}(q)$ is the pulse-transfer function from the control action to the other part of the error signal:

$$y(k) = T_{ce}(q)f_c(k).$$

Consider the input-output relation between the control force as the output of the adaptive filter $W(z,k)$ and seismic disturbance input:

$$f_c(k) = W(q,k)\ddot{x}_g(k).$$

For comparison, the above equation in the z-domain (or q^{-1}-domain) is equivalent to the following convolution

sum in the time-domain:

$$f_c(k) = \sum_{j=0}^{L} w(j,k)\ddot{x}_g(k-j).$$

In the above equation, $w(j,k) = w_j(k)$ is the jth weight of discrete-pulse response of adaptive filter, determined for the sampling period k.

The objective in adaptive control is to calculate $W(z)$ filter weights optimally, i.e., w_j at each time step k.

The relation of $W(z,k)$, the adaptive controller, and its jth Markov parameter, $w(j,k)$ (or jth weight of discrete pulse response of that filter), in the z-domain is written as:

$$W(z,k) = \sum_{j=0}^{L} w_j(k) z^{-j},$$

$W(z,k)$ is an FIR (Finite Impulse Response) filter that can be truncated after L time points for the adaptive controller. Implying that the optimization space dimension is $(L+1)$. w_j's, at each sampling time k, are the design variables.

Through combining the above relations, the following relation is obtained:

$$y(k) = T_{ce}(q) \sum_{j=0}^{L} w_j(k) q^{-j} \ddot{x}_g(k).$$

The error signal is found in terms of structural transfer functions as:

$$e(k) = T_{de}(q)\ddot{x}_g(k) + T_{ce}(q) \sum_{j=0}^{L} w_j(k) q^{-j} \ddot{x}_g(k).$$

A filtered sequence of acceleration seismic signal through structural transfer function is defined by:

$$\ddot{\tilde{x}}(k) = T_{ce}(q)\ddot{x}_g(k).$$

Substituting the filtered signal into the error signal, the following relation is obtained:

$$e(k) = T_{de}(q)\ddot{x}_g(k) + \sum_{j=0}^{L} w_j(k)\ddot{\tilde{x}}(k-j).$$

The above relation has been written by the use of backward-shift operator property:

$$q^{-j}\ddot{\tilde{x}}(k) = \ddot{\tilde{x}}(k-j).$$

Mean square of error signal is chosen as an objective function for determining the optimal values of $w_j(k)$, Markov parameters of the $W(z,k)$ filter at time k:

$$C(w_j(k)) = \mathbf{E}\{e^2(k)\} \quad j = 0, ..., L.$$

Calculating the gradient of the above cost function relative to the adaptive filter coefficients, it is obtaind that:

$$\frac{\partial C(w_j(k))}{\partial w_j(k)} = \mathbf{E}\left\{2e(k)\frac{\partial e(k)}{\partial w_j(k)}\right\}.$$

The approximation of this deterministic gradient converging theoretically to Wiener filter solution, by a stochastic gradient, yields the so-called Single-Channel Least-Mean-Square (LMS-SISO) algorithm:

$$\frac{\partial C(w_j(k))}{\partial w_j(k)} \cong 2e(k)\frac{\partial e(k)}{\partial w_j(k)}.$$

Using this gradient, the general recursive updating formula of steepest descent, given by:

$$w_j(k+1) = w_j(k) - \gamma \frac{\partial C(w_j(k))}{\partial w_j(k)},$$

is specialized to the following difference equation for filter weights update in LMS algorithm:

$$w_j(k+1) = w_j(k) - 2\gamma e_i(k)\frac{\partial e_i(k)}{\partial w_j(k)}.$$

The sensitivity derivatives are calculated by differentiating the error signal:

$$\frac{\partial e(k)}{\partial w_j(k)} = \ddot{\tilde{x}}(k-j) \quad j = 0, ..., L.$$

The final result of the filtered-x LMS algorithm, SISO case, is:

$$w_j(k+1) = w_j(k) - 2\gamma e(k)\ddot{\tilde{x}}(k-j), \quad j = 0, ..., L.$$

The major difficulty of filtered-x version of LMS algorithm is to estimate structural transfer function $T_{ce}(z)$ for obtaining filtered seismic signal. This can be accomplished by having a rough finite element reference model of the structure:

$$\ddot{\tilde{x}}(k) \cong \hat{T}_{ce}(q)\ddot{x}_g(k).$$

The above derivation with fewer indexes for quantities was for SISO filtered-x LMS algorithm. The Multi-Input Multi-Output (MIMO) filtered-x LMS case with three inputs and three outputs has been organized in the main body of the paper.

The concepts of z-transform, FIR filters and other terminology related to DSP (Digital Signal Processing) may be found in [24,27]. The concepts like LMS and other terminology related to RSP (Random Signal Processing), stochastic processes and ASP (Adaptive Signal Processing) fields may be found in [21,22].